SLAC–PUB–4961
April 1989
(T/E)

AN ALIGNMENT METHOD FOR THE MARK II SILICON STRIP VERTEX DETECTOR USING AN X-RAY BEAM*

CHRIS ADOLPHSEN, GIORGIO GRATTA, LUIS LABARGA, ALAN LITKE,
ANDREAS SCHWARZ, MICHAL TURALA‡ AND CARLA ZACCARDELLI
Santa Cruz Institute for Particle Physics,
University of California, Santa Cruz, CA 95064

ALAN BREAKSTONE AND SHERWOOD PARKER
University of Hawaii, Honolulu, HI 96822

BRUCE BARNETT, CHRIS BOSWELL, PAUL DAUNCEY, DAVID DREWER,
JOHN MATTHEWS AND STEVE VEJCIK
Johns Hopkins University, Baltimore, MD 21218

ROBERT JACOBSEN AND VERA LÜTH
Stanford Linear Accelerator Center, Stanford University, Stanford, CA 94309

ABSTRACT

A silicon strip vertex detector consisting of 36 independent detector modules is being constructed for use in the Mark II detector at the SLAC Linear Collider. This paper describes a method for determining the relative alignment of the modules to a precision better than the 5 μm intrinsic resolution of the detectors. The basic procedure involves moving the vertex detector by known amounts through a fixed, collimated X-ray beam, and using the beam position reconstructed from the detected signals to determine the relative positions and orientations of the modules. Results from tests of the method on a subset of detectors are presented.

*Work supported by Department of Energy contracts DE–AM03–76SF00010, DE–AA03–76SF00034 and DE–AC03–83ER–40103.

‡Visitor from the Institute of Nuclear Physics, Krakow, Poland.

Presented at the 5th European Symposium on Semiconductor Detectors, Munich, W. Germany, February 21–23, 1989.

1. INTRODUCTION

To provide the Mark II detector with a precision tracking capability for the study of short lived particles, we are constructing a silicon strip vertex detector [1]. It consists of 36 independent detector modules housed in two hemicylindrical structures that attach to the beam pipe at the interaction region. The modules are grouped into three radial layers of radii 28, 33 and 37 mm with strip spacings of 25, 29 and 33 μm, respectively (see fig. 1). The strips are oriented parallel to the beam axis and hence track position is measured only in the r–ϕ plane; the central drift chamber provides the z track information. The detecting element in each module is a single-sided, 512-strip silicon detector of 300 μm thickness. It is read out with four custom 128-channel VLSI chips (the "Microplex") that integrate and store the charge collected on each strip and multiplex the analog signals onto a serial bus [2]. The chips are wire bonded to both ends of the detector as shown in fig. 2. The module also contains a hybrid circuit which provides control signals, a switchable capacitor bank for power, and an amplifier and line driver for the output signals.

Tests of the modules in a fixed target geometry have yielded position resolutions of less than 5 μm. To achieve a comparable impact parameter resolution with the detectors configured in a cylindrical geometry requires much more effort. Our general approach is to use the module support structure to place the strips to a coarse accuracy ($\approx$ 50 μm), and to use other techniques to more precisely ($\approx$ 2 μm) measure their location. The coarse alignment level is set so the 2 mm z resolution of the central drift chamber does not significantly worsen the $r\phi$ detector resolution because of misalignment of the strips relative to the z axis.

A prototype of one of the two hemicylindrical structures built to house the modules is shown in fig. 3. The inner shell of each unit attaches to the beam pipe by a three point mounting system. The slots in the endplates are used to support the modules and are cut using electrodischarge machining. Once inserted into the slots, a module is held in place by spring fixtures which are attached to each end of the module. The inner and outer shells, which provide the structural rigidity, are made of 250 μm-thick beryllium, and the endplates are made of aluminum.

To determine the locations of the modules in the support structure, we use two methods. The first is based on coordinate measurements of the surfaces of the detectors that are made with a precision microscope measuring system. The data are taken as each layer is loaded; the outer shell remains detached so the detector strips can be fully viewed. After these measurements are complete and the outer shell attached, alignment measurements begin using a collimated X-ray beam. The advantage of this method is that the beam can penetrate the shells and the detectors so the measurements can be made after assembly is complete. The remainder of this paper describes the method in detail.

2. ALIGNMENT EQUATIONS

To formulate the equations that describe the alignment problem, we consider a single detector in a reference frame where its strips are parallel to the z axis and perpendicular to the x axis, as shown in fig. 4. Let the detector be centered about $x = 0$ but displaced vertically by y_o to represent its radial position in the module support structure. Relative to this nominal location, there are five degrees of freedom describing its possible misalignment. To represent these, we choose the translational displacements Δx and Δy of the center of the detector, and the rotational angles $\Delta\eta$, $\Delta\theta$ and $\Delta\phi$ about the body of the detector, as shown in the figure. If we assume all displacements are small, then the order of the translations and rotations describing the misalignment is irrelevant. The effect of misalignments can be seen through a comparison of a track position measured by the detector ($\equiv x_m$) with the position expected from an independent measure of the track trajectory. By a track, we assume for simplicity a straight line trajectory and use as a parameterization its intercepts in the x–z plane, x_b and z_b, and its slopes relative to the y axis, $tx_b \equiv dx/dy$ and $tz_b \equiv dz/dy$. In the absence of misalignments and measurement error, the following relation holds:

$$\Delta x_m \equiv x_m - x_b - y_o \cdot tx_b = 0 \quad .$$

With the inclusion of the misalignment degrees of freedom, the first-order difference between the measured and expected track position becomes

$$\begin{aligned} \Delta x_m = & -\Delta x + \Delta y \cdot tx_b - \Delta\eta \cdot (z_b + y_o \cdot tz_b) + \\ & \Delta\theta \cdot tx_b \cdot (z_b + y_o \cdot tz_b) + \Delta\phi \cdot tx_b \cdot (x_b + y_o \cdot tx_b) \quad . \end{aligned}$$

By recording track positions reconstructed in the detector and independently knowing the track parameters, the offsets, Δx, Δy, $\Delta\eta$, $\Delta\theta$ and $\Delta\phi$ can be estimated in a least-squares fit using the above equations. Other variables can also be included in the fit to account for any mechanical deformation of the detectors, such as bowing and twists.

3. ALIGNMENT MECHANICS

To apply this method, we use a beam of collimated X-rays instead of particles. With a particle beam, the detector is normally held stationary and tracks are measured in an external telescope system. We, however, fix the X-ray beam and move the detector. The position and orientation of the vertex detector is controlled by the system of stages shown in fig. 5. The cylindrical structure in the photo is a mock-up of the beam pipe segment on which the module support structure attaches. The pipe is connected to a rotation stage whose base is mounted on a linear stage that moves parallel to the vertical axis. In the coordinate notation of fig. 4, these are the ϕ and y stages. This assembly is attached to a linear stage that moves in x, which itself is mounted on a stage that moves in z.

The combined set of stages provides individual control of the x, y, and z positions of the modules and their ϕ orientation about the rotation axis of the dummy beam pipe. Each stage is driven by a computer-controlled stepping motor and can be positioned with an accuracy of 1 to 2 μm.

In the alignment equations described above, the detector is considered to be stationary and the track trajectories vary. We keep the same formalism by translating the changes in the stage settings to equivalent changes in the X-ray beam trajectory. To do this, an absolute coordinate system has to be defined in the reference frame of the stages. For convenience, the rotation axis, which is assumed to be parallel to the z axis, is chosen as the origin of the x–y plane. The stage settings are referenced to some initial configuration of the modules with respect to the beam. To make the geometry simple and the misalignment offsets small, the zeroes of the stage settings are chosen for a configuration where the beam is roughly centered on a given detector (the beam positions measured by the detectors are also referenced relative to the center strip). The other detectors can then be similarly positioned with only a ϕ rotation, and their misalignments measured in the same reference frame. The z origin in this system is set at an arbitrary point near the middle of the detectors. This degree of freedom is a result of the translational invariance in z and it allows the initial z intercept of the beam to be defined as zero. For the x axis, the rotations in ϕ break the translational symmetry so the x intercept of the beam ($\equiv x_o$) needs to be known. The beam angles are also needed in both the x–y plane ($\equiv \phi_o$) and the y–z plane ($\equiv \theta_o$). The method used to determine these quantities will be described later. With these three values, the beam parameter terms in the alignment equations are computed from the stage settings, x_s, z_s and ϕ_s, by

$$\begin{aligned} x_b &= \alpha \cdot (x_s + x_o) \\ tx_b &= \tan(\phi_s + \phi_o) \\ z_b &= z_s \\ tz_b &= \tan(\theta_o) \end{aligned}$$

where

$$\alpha = \cos(\phi_s) + \sin(\phi_s)\tan(\phi_o + \phi_s) \quad .$$

These equations complete the set needed to do the alignment fits.

4. X-RAY SOURCE

The other major component of the alignment apparatus is the X-ray source. We use a conventional X-ray tube with a water-cooled target (anode) [3]. In the alignment tests, targets of tungsten and molybdenum have been used. During operation of the tubes, an electron current flows a few millimeters from a heated filament, which is at high voltage, to the grounded target. X-rays are produced from atomic transitions (characteristic lines) and bremsstrahlung (continuum) when the electrons interact with the target material. The continuum intensity, I, depends on the atomic number of the material ($I \propto Z$) and on the voltage applied ($I \propto V^2$). The X-ray tubes we use can be operated at a potential up to 60 kV. The X-ray intensity is limited by the 1.5 kW power ratings of the tubes which can only be run in a continuous mode.

The choice of the target material was dictated in part by the need to produce X-rays of energies that readily penetrate the module layers, and of intensities sufficient to compensate for losses due to collimation and the duty factor of the module read out. As a measure of the energies of interest, a 12.9 keV X-ray has an absorption length in silicon equal to the thickness of our detectors (300 μm). Between 2 and 40 keV, the absorption length increases roughly exponentially with energy by about four orders of magnitude. The larger absorption cross section at low energy yields a larger detector signal per incident X-ray, but creates problems for the alignment measurements. One is a large bias in the reconstructed beam position for non-normal beam incident angles because the beam interaction rate in silicon decreases with depth. Corrections for this effect could be made, but they would require a detailed knowledge of the X-ray energy spectrum. Another problem arises from the changes in the X-ray intensity that would have to be made when measuring detectors in different layers. The concern is that these adjustments could lead to systematic shifts in beam position. Given these effects, one wants a spectrum in which the low energy X-rays can be attenuated while maintaining a reasonable signal size from the high energy X-rays. For a given spectrum, such a trade-off is best achieved by using filters made of low Z elements such as aluminium, which have both a steep and a continuous absorption function for low energy X-rays.

In choosing an X-ray tube, we considered target elements whose characteristic lines are either at low energies where they can be readily filtered, or at high energies where the absorption lengths are larger than the silicon thickness, but not so large that the contribution to the signal from these X-rays is small. The tungsten tube falls in the former category where the dominate resonant X-rays are the L lines at about 10 keV if the tube is operated below 60 kV. As an illustration of the spectral characteristics of such a tube, fig. 6 shows a plot of the signal from a silicon detector as a function of the energy of the X-rays. The distribution was calculated using spectral distribution data from a similar X-ray tube which was operated at 45 kV [4]. The calculation takes into account the detection efficiency in silicon and assumes the X-rays are filtered by 0.8 mm of aluminum. For our alignment measurements, we will use the tungsten tube operated at a larger potential (60 kV) to produce both a larger beam intensity and average beam energy. The beam will also be filtered as in the above example which reduces the position bias to less than 2 μm at the largest beam angles, and decreases the attenuation in signal size from the outer to the inner layer to a factor of 1.9. Another reasonable choice of target material is molybdenum where the ≈ 20 keV characteristic K lines increase the signal size but yield a somewhat larger position bias and signal attenuation per layer.

The X-ray tubes we use were designed for diffraction studies where the spot size of the electron beam at the target is small in one dimension. For the tungsten tube, this spot size is 0.4 mm by 8 mm. The X-rays exit the tube at 6° angles to the target surface through four ports with beryllium windows. Two of the ports are aligned parallel to the long dimension of the electron beam and two are perpendicular to it. For our measurements, we use one of the two former ports which effectively reduces the long dimension of the spot size to 0.8 mm due to the projection angle.

Figure 7 shows a photo of the stage assembly in place under the X-ray source with one of the module support structures attached to the dummy beam pipe. The rectangular structure at the top of the photo contains the X-ray tube. The modules installed in the housing in this case are mechanical prototypes. The flexible cables in the photo are similar to the actual ones which carry control signals to individual modules. They enter from only one end of the housing and are held in place by a fixture that attaches to the dummy beam pipe.

The cylindrical structure that extends below the X-ray tube housing in fig. 7 collimates the beam emerging from the bottom port of the X-ray tube. It is a hollow brass tube with a pair of 3 mm-thick tungsten slits attached to the bottom end. The slits have a 50 μm by 2 mm opening and are oriented so the larger opening is in the direction parallel to the detector strips. The slits are covered by a piece of 0.8 mm-thick aluminum sheet that serves as a filter. The distance between the collimator and the target is set to be roughly ten times the separation between the inner and outer module layer. With the outer shell of the module support structure positioned a few millimeters below the collimator, and the X-ray tube oriented so the narrower dimension of the production spot size is perpendicular to the detector strips, a beam width of less than 100 μm is produced at all three layers in the dimension transverse to the strips.

5. BEAM RECONSTRUCTION

During the read out of a module, the analog output signals are sent to an "intelligent" digitizer (the BADC) [5]. For each sample of the beam, 100 events are recorded at a rate of 20 Hz and the pulse heights for each strip are averaged. The integration gate width for each event is 1 μsec so the read out duty factor is only 2×10^{-5}. A typical example of a beam measurement is shown in fig. 8. Here, the pulse height is plotted as function of strip number in the region of the detector exposed to the beam. The detector in this case was in the outer layer and was located about 1 cm below the collimator. The X-rays were generated in the tungsten tube which was operated at a 60 kV potential and a 20 mA electron current. To set the pulse height scale in the figure, the most probable energy loss of a minimum ionizing particle in the detector (84 keV) corresponds to 80 ADC units, and the rms noise of a single channel (per sample) is about 0.4 ADC units. The peak pulse height in the figure is thus about 400 times the single channel rms noise.

The pedestals for the data in fig. 8 were obtained by averaging 300 events (three samples) with the beam off. A gain correction has been applied to each channel that was computed from data taken using a 2 mm-diameter circular collimator to generate a broad width X-ray beam. The data were recorded at 200 evenly-spaced positions across the width of the detector to produce a uniform exposure of each strip to X-rays. The pulse heights from each channel that exceeded a certain threshold were averaged to yield a measure of the gain of that channel. In general, the gains for the strips read out on a given end of a detector have an rms variation of about 4% but can be systematically shifted from those on the opposite end by up to 30%. The reason for these differences is not understood.

The width of the beam in fig. 8 is roughly as expected given the broadening that occurs from the $\approx$ 10% capacitive coupling between strips. The smearing due to the range of the photoelectrons produced in the silicon (< 20 μm) and the diffusion of the collected charge (< 4 μm rms) is relatively small. The beam position is determined by a centroid calculation that includes the five strips on either side of the strip with the maximum pulse height. As a measure of the position resolution achieved with this method, repeated beam measurements were made and the rms of their variation was computed. The result is 0.7 μm, and includes the effect of any beam position instability during the half hour of data taking.

6. ALIGNMENT MEASUREMENTS

Before the alignment procedure begins, a number of measurements are done to check the linearity and calibration of the stages. For example, the x stage is checked by moving a detector through the beam using this stage, and fitting the reconstructed beam position as a function of stage location. Figure 9 shows the residuals for a linear fit to data taken when an outer layer module was moved through the beam in 60 steps. The rms of the residuals is 1.1 μm for the $\approx$ 16 mm distance of travel. This value is a measure of the convolution of the stage placement accuracy and the beam reconstruction resolution. The slope determined from the fit is equal to unity to within a part in 10^4 which verifies to this level both the scale of the stage and the assumed strip spacing. A separate calibration of the x stage using a precision depth gauge gives similar results in scale and linearity.

The other stages have been checked by similar methods. The z stage, which has a coarser position control, has a location accuracy of about 2 μm and shows no discernible "wobble" in x during its movement. The accuracy of the rotation stage in $r\phi$ at the radii of the modules is about 1.5 μm. Its scale was verified by the reproducibility of the measured beam position upon 360° rotations.

Another issue in preparing the apparatus for alignment measurements is the orientations of the stages. In deriving the alignment equations discussed earlier, it was assumed that the x, y and z stages are orthogonal, and that the rotation axis is parallel to the z axis. A study of the sensitivity of the alignment results to systematic errors in these orientations shows that the orthogonality of the three linear stages has to be known to about 1 mrad. The parallelism of the rotation and z axis in the x–z plane, however, has to be known to better than 0.1 mrad. To measure the orthogonality of the axes, we use the "touch point" coordinate measurement facility at SLAC. It has a measurement accuracy of about 0.2 mrad for our application. The angular misalignments measured are on the order of 1 mrad, and are used to correct the stage position data when doing the alignment fits.

The parallelism of the rotation and z axis is determined from a set of measurements that is also used to determine the x intercept of the beam (x_o). As discussed earlier, x_o is one of the three beam parameters that enter the alignment equations that have to be measured. The data are taken by picking a reference position on a detector and moving both the x and ϕ stages in a series of steps so that the beam stays at the reference location on the detector. The ϕ positions are set within a range of $\pm$ 30°, and the x positions are adjusted accordingly [$x \approx y_o \sin(\phi)$]. The exact relation between x and ϕ depends on the initial x and y location of the detector reference point and on the beam intercept. A fit to these data allows one to extract x_o. The goodness of fit also confirms the rotation stage linearity over a 60° range. Measuring x_o at different z locations yields the angle between the rotation and z axis in the x–z plane. For the parallelism in the y–z plane, both the tolerance and the method of measurement are the same as that for the orthogonality of the axes.

The final quantities measured in preparation for alignment data taking are the beam angles tx_b and tz_b. The slope in the x–y plane is obtained from data taken by moving the y stage in a series of steps over a 1 cm range. The error on the slope from this measurement is better than the accuracy to which y stage orientation is known. Reorienting the set of stages by 90° in the x–z plane and repeating the measurements yields tz_b. In this case the beam is much wider, but the required measurement precision is also larger. The orientation of the X-ray tube housing is adjusted so that the beam angles are less than 1 mrad in each plane.

With these measurements complete, alignment data are taken for one module at a time. Each detector is first centered below the collimator using the rotation stage. The ϕ angle is recorded and defines the nominal orientation of the module about which the misalignments are measured. A sequence of scans as shown in fig. 10 is then done at five z locations. This takes about 30 minutes to complete and is done totally under computer control. For each z position, data are taken at three x locations (near channels 30, 256 and 482) for three rotations settings (−200, 0 and 200 mrad). This "parallax" view of the detector at a given z location measures its displacement (Δx and Δy) and tilt ($\Delta\phi$). The variation of the displacements with z determines $\Delta\eta$ and $\Delta\theta$. The five misalignments are in fact computed in a single fit to the 45 measurements using the equations discussed earlier. The fit also includes terms representing the stage position uncertainties so that this source of error is properly incorporated. Figure 11 shows the distribution of the residuals from a measurement of an outer layer detector. The rms of the data is 1.8 μm which corresponds to an alignment precision that meets our requirements. Measurements of detectors in other layers yield similar rms values. The misalignments computed in these cases verify that the modules are placed in the housing to within our coarse alignment tolerance.

7. SUMMARY AND OUTLOOK

We have presented a method for measuring the relative locations of the modules in our silicon strip vertex detector using a collimated X-ray beam and a set of high precision stages. This technique makes it possible to achieve an alignment precision of about 2 μm. Currently, we are doing tests of the alignment system to check for systematic errors and to measure the stability of the modules in the support structure. We are also comparing results from the X-ray and optical measurements of a subset of detectors. We hope to begin full scale measurements of the first hemicylinder shortly.

ACKNOWLEDGMENTS

We thank Pierre Capeder, Glen Kerr, Hans Przybylski, W. Hal Tompkins and Teresa Troxel of the Stanford Synchrotron Radiation Laboratory for their generous support of this project.

REFERENCES

[1] C. Adolphsen *et al., IEEE Trans. Nucl. Sci.,* **NS–33** (1986) 57; *Nucl. Instr. and Meth.,* **A235** (1987) 444; *IEEE Trans. Nucl. Sci.,* **NS–35** (1988) 424.

[2] J. T. Walker *et al., Nucl. Instr. and Meth.,* **226** (1984) 200;
G. Anzivino *et al., Nucl. Instr. and Meth.,* **A243** (1986) 153.

[3] The X-ray generator (model XRG 3100) and tubes we use are manufactured by Philips.

[4] J. V. Gilfrich, "Handbook of Spectroscopy," Vol. I, CRC Press (1974) 232.

[5] M. Breidenbach *et al., IEEE Trans. Nucl. Sci.,* **NS–25** (1978) 706.

FIGURE CAPTIONS

Fig. 1. The layout of the silicon strip vertex detector.

Fig. 2. The plan for a silicon detector module.

Fig. 3. Prototype of the mechanical support structure for the modules. The outer shell is shown detached from the endplate and inner shell assembly.

Fig. 4. A detector and the coordinate system used to describe misalignment. The detector strips are parallel to the z axis.

Fig. 5. System of stages (three linear and one rotation) used to vary the position and orientation of the vertex detector for the alignment measurements. The cylindrical structure is a mock-up of the beam pipe segment on which the module support structure attaches.

Fig. 6. Signal from a silicon detector as a function of the energy of the X-rays. The calculation assumes the X-rays are generated by a tube with a tungsten target that is operated at 45 kV, and that the beam is filtered by 0.8 mm of aluminium. The peaks near 10 keV are the characteristic L lines of tungsten.

Fig. 7. Alignment measurement setup including the stages, dummy beam pipe, module housing, X-ray beam collimator and X-ray tube housing. The modules installed in the housing are mechanical prototypes.

Fig. 8. Pulse height versus strip number in the region of a detector exposed to the X-ray beam. Each strip is 33 μm wide.

Fig. 9. Residuals from a linear fit to measured beam position versus x stage position data plotted (a) as a function of the stage position and (b) in a histogram.

Fig. 10. Sequence of scans done at five z locations in the alignment measurement procedure. The vertical arrow and thick cross bar represent the X-ray beam and detector respectively. The point where the narrow lines cross is the rotation axis.

Fig. 11. Residuals from the fit for the five misalignment degrees of freedom for an outer layer module.

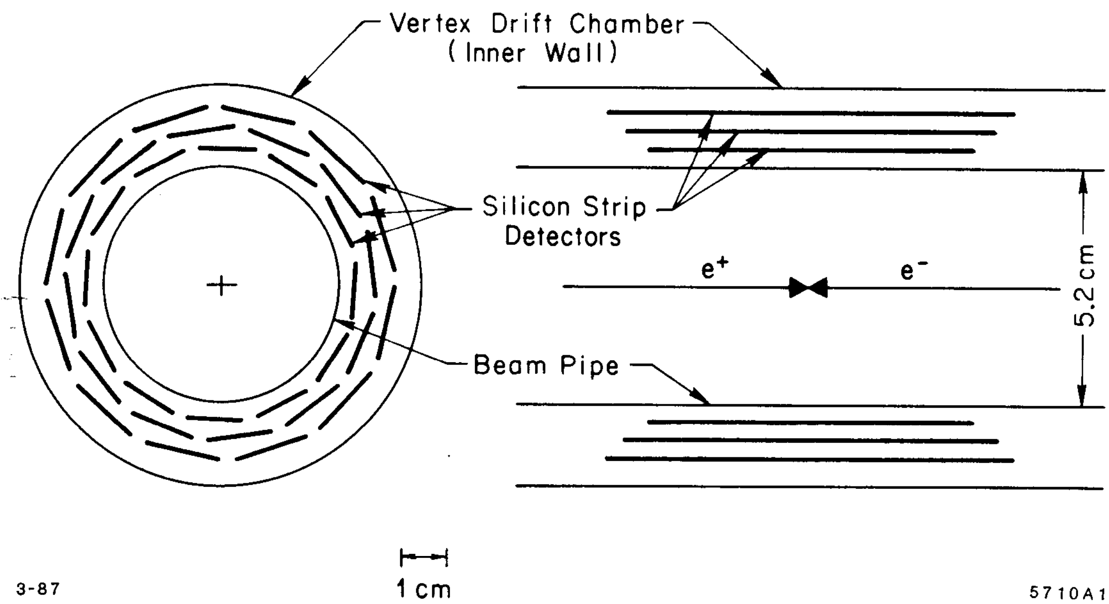
Vertex Drift Chamber
(Inner Wall)
Silicon Strip
Detectors
e^+
e^-
5.2 cm
Beam Pipe
1 cm
3-87
5710A1

Fig. 1

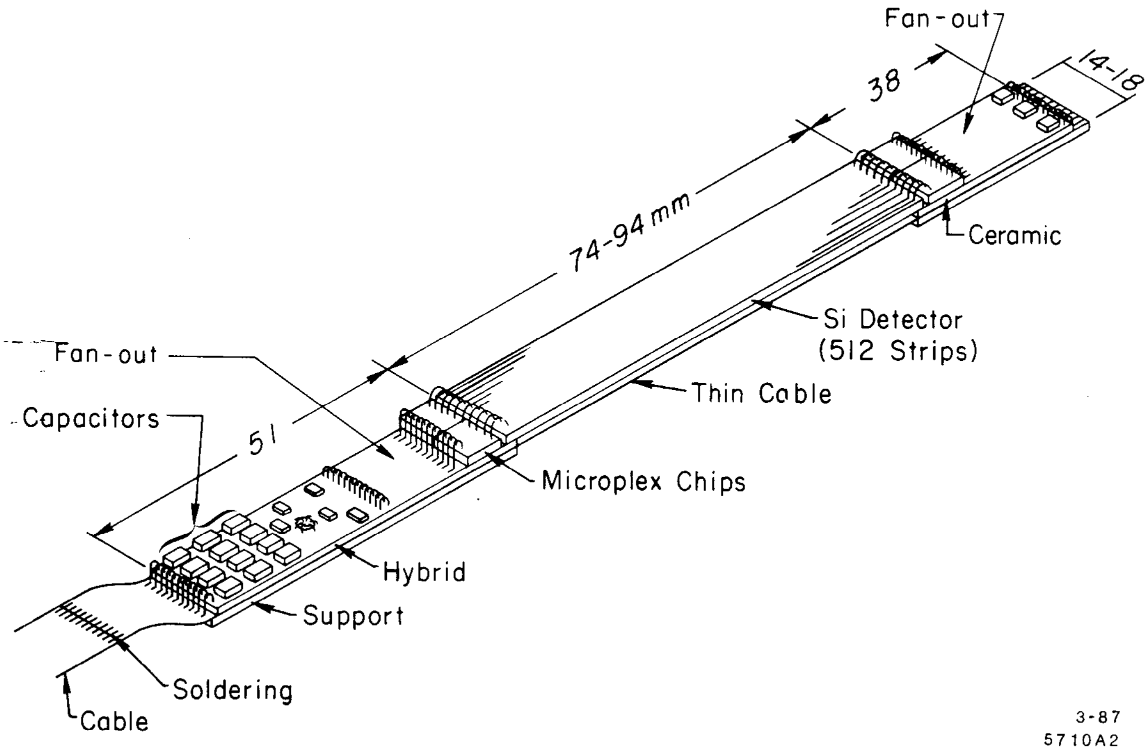
Fan-out
38
14-18
74-94 mm
Ceramic
Si Detector
(512 Strips)
Fan-out
Thin Cable
Capacitors
51
Microplex Chips
Hybrid
Support
Soldering
Cable
3-87
5710A2

Fig. 2

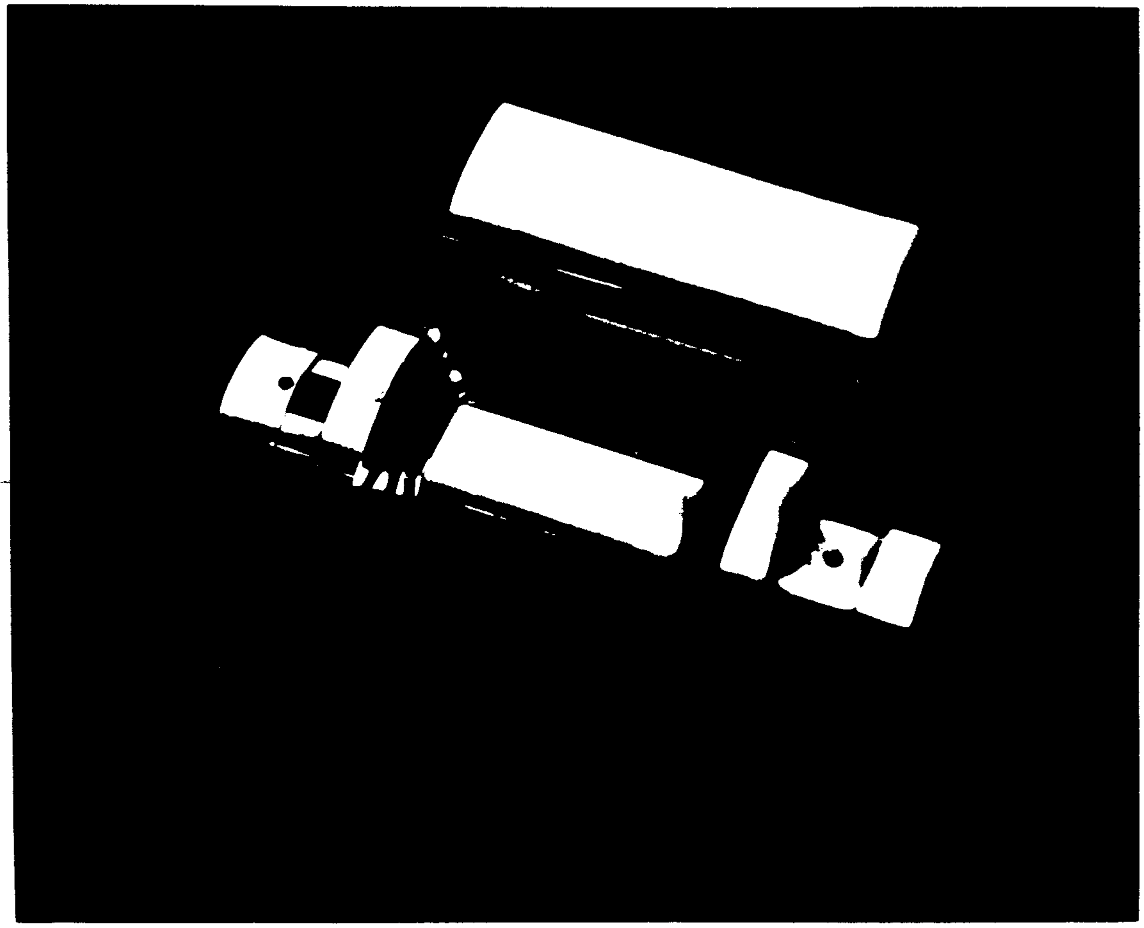

Fig. 3

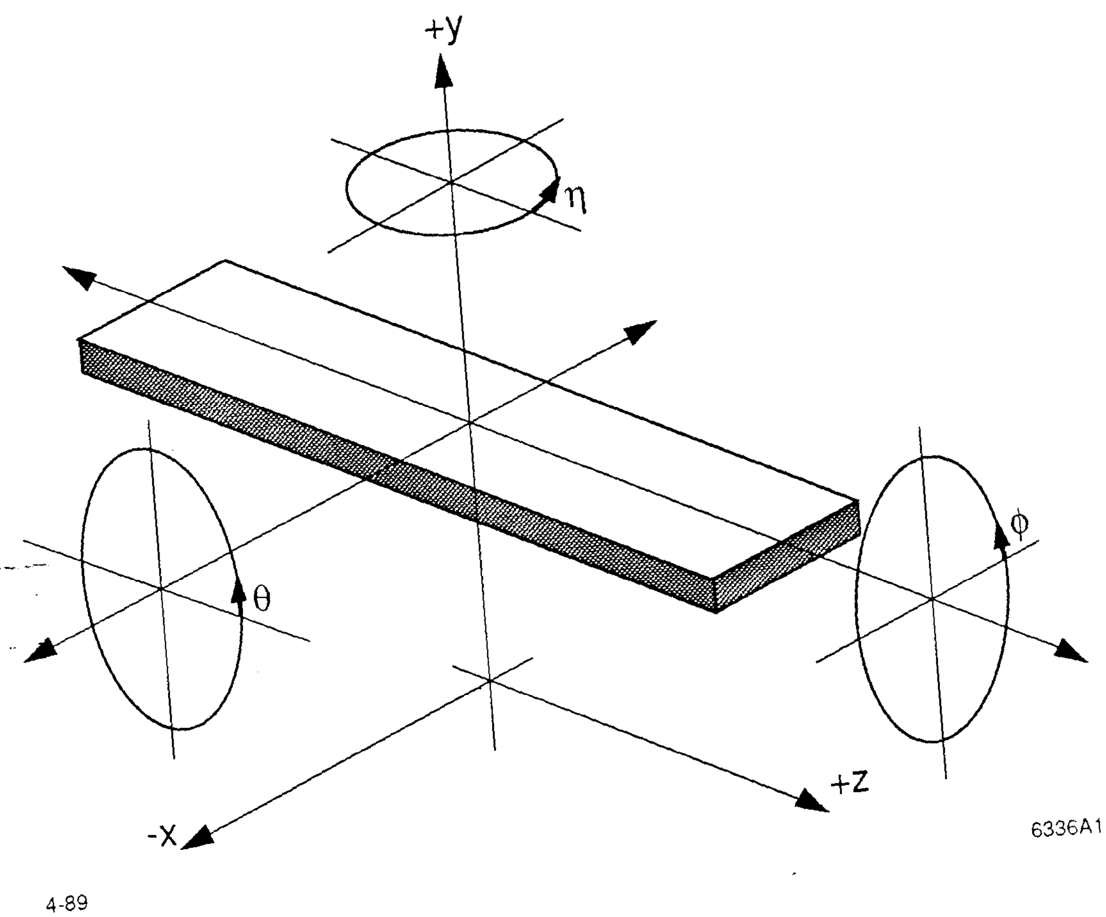

Fig. 4

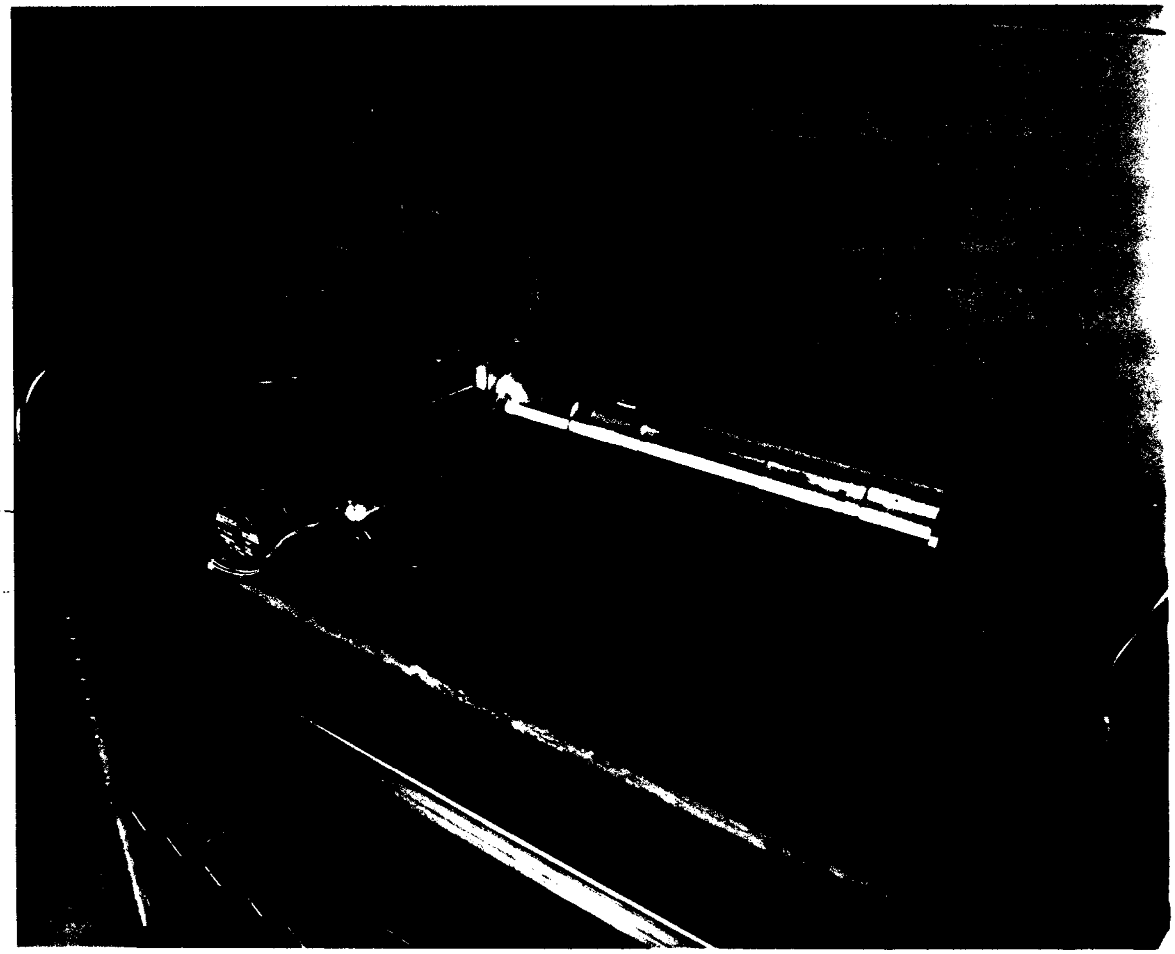

Fig. 5

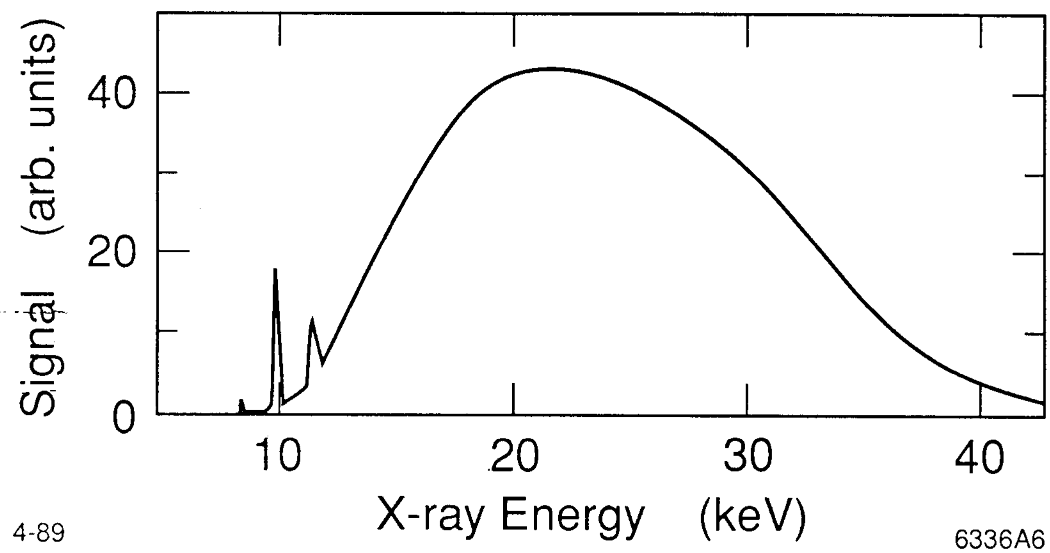

Fig. 6

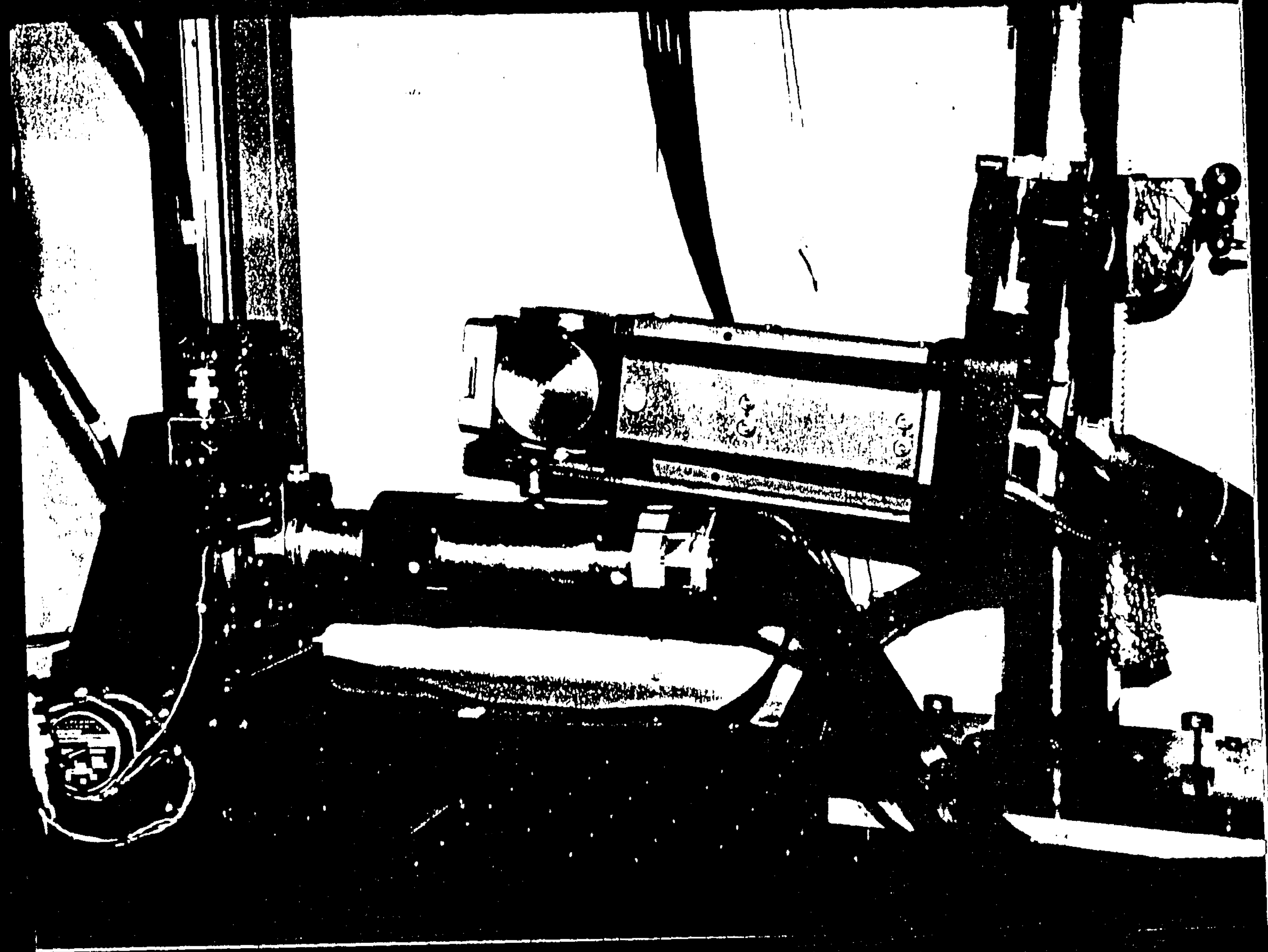

Figure 2: Alignment measurement setup including the stages, module housing, X-ray beam collimator and X-ray tube and housing. The modules installed in the support structure are mechanical prototypes.

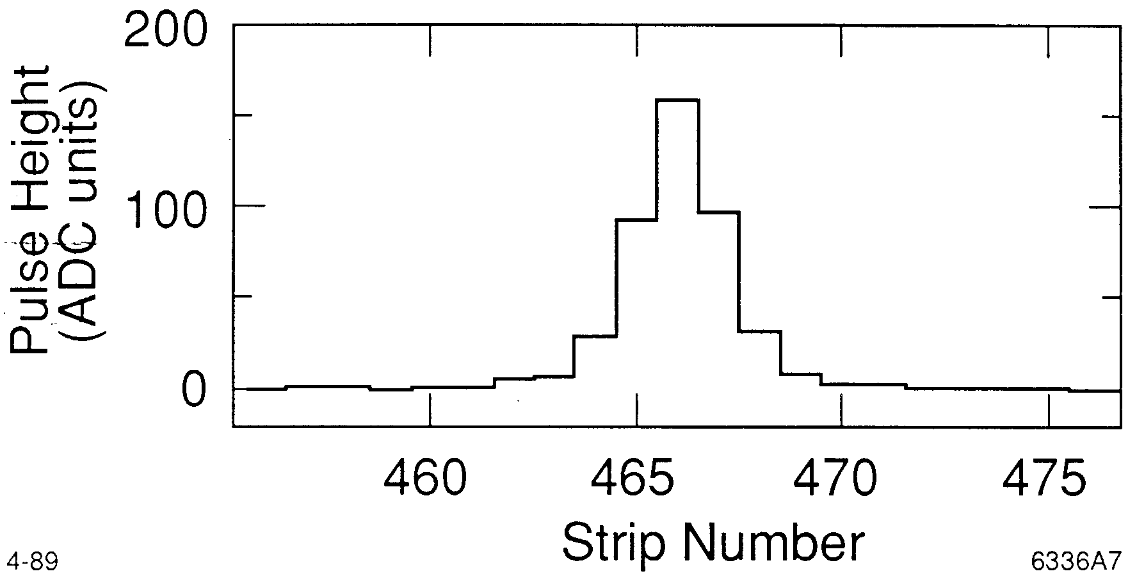

200
100
0
Pulse Height (ADC units)
460
465
470
475
Strip Number
4-89
6336A7

Fig. 8

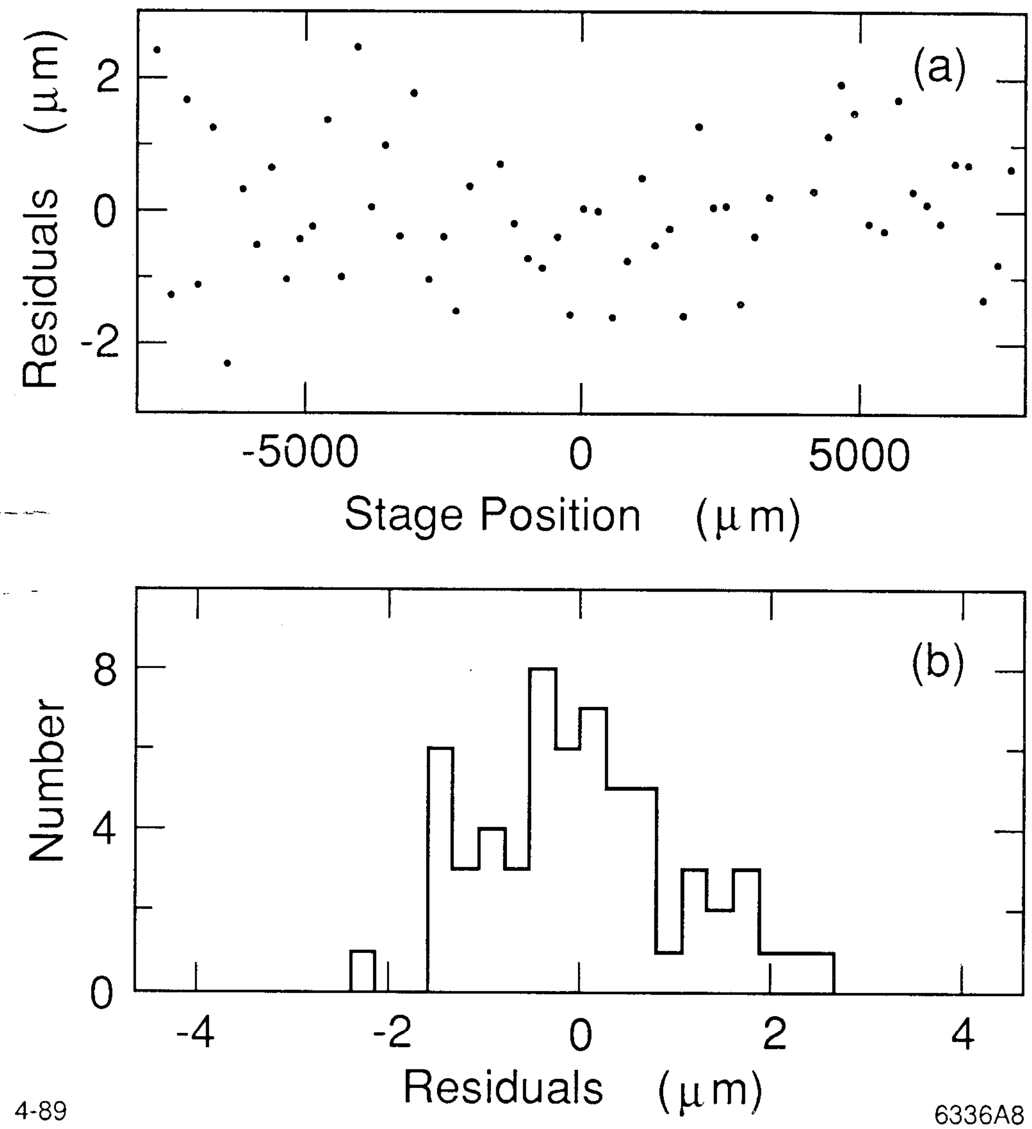
(a)
Residuals (μm)
2
0
-2
-5000
0
5000
Stage Position (μm)
(b)
Number
8
4
0
-4
-2
0
2
4
Residuals (μm)
4-89
6336A8

Fig. 9

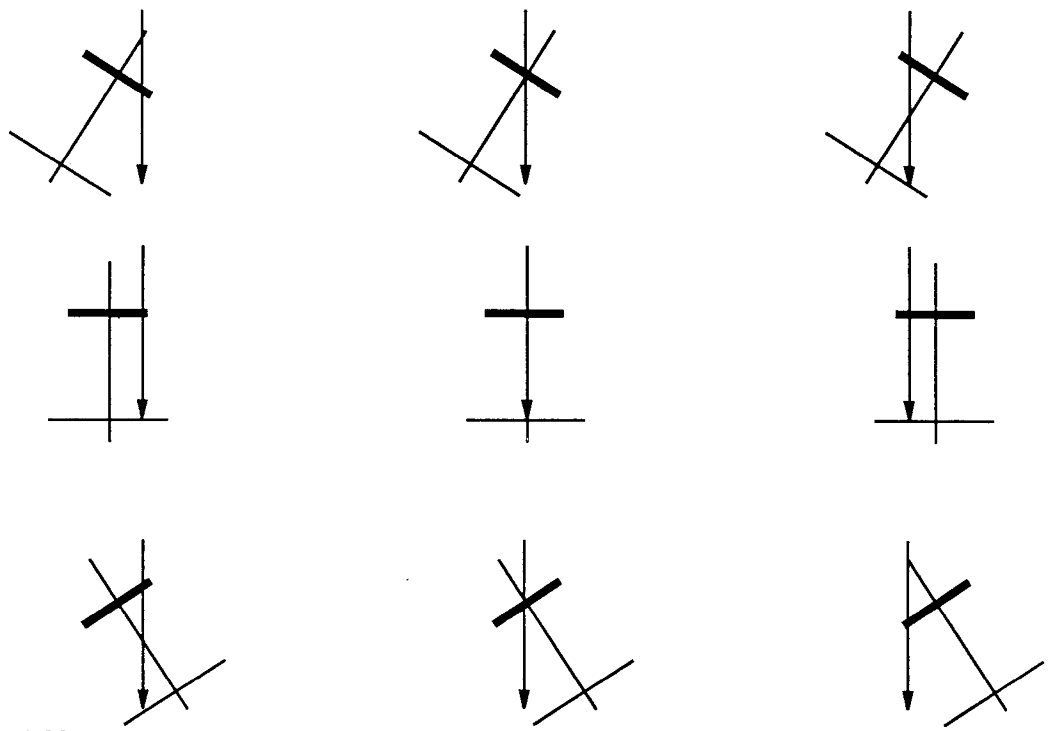

4-89
6336A9

Fig. 10

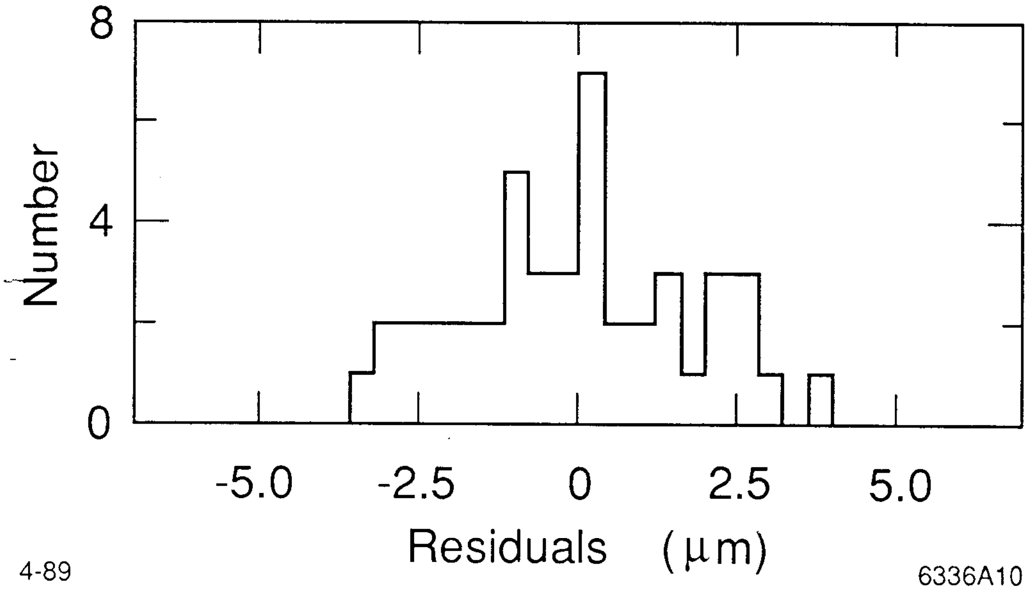

Fig. 11